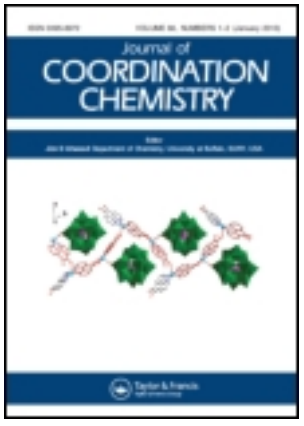

Journal of Coordination Chemistry
Publication details, including instructions for authors and subscription information:
http://www.tandfonline.com/loi/gcoo20

Synthesis, structure, spectroscopic, and DNA binding properties of Co(III) and Ni(II) complexes with ((E)-2-(amino((pyridin-2-ylmethylene)amino)methylene)maleonitrile

Bing Li [a], Wei Liu [b], Jia Shao [a], Chun-Lan Xue [a], Cheng-Zhi Xie [a], Yan Ouyang [a] & Jing-Yuan Xu [a]

[a] Tianjin Key Laboratory on Technologies Enabling Development of Clinical Therapeutics and Diagnostics, School of Pharmacy, Tianjin Medical University, Tianjin, P.R. China

[b] The Second Hospital of Tianjin Medical University, Tianjin, P.R. China

Accepted author version posted online: 22 May 2013.Published online: 21 Jun 2013.

To cite this article: Bing Li, Wei Liu, Jia Shao, Chun-Lan Xue, Cheng-Zhi Xie, Yan Ouyang & Jing-Yuan Xu (2013) Synthesis, structure, spectroscopic, and DNA binding properties of Co(III) and Ni(II) complexes with ((E)-2-(amino((pyridin-2-ylmethylene)amino)methylene)maleonitrile), Journal of Coordination Chemistry, 66:14, 2465-2476, DOI: 10.1080/00958972.2013.807341

To link to this article: http://dx.doi.org/10.1080/00958972.2013.807341

Journal of Coordination Chemistry, 2013
Vol. 66, No. 14, 2465–2476, http://dx.doi.org/10.1080/00958972.2013.807341

Synthesis, structure, spectroscopic, and DNA binding properties of Co(III) and Ni(II) complexes with ((*E*)-2-(amino ((pyridin-2-ylmethylene)amino)methylene)maleonitrile)

BING LI†[1], WEI LIU‡[1], JIA SHAO†, CHUN-LAN XUE†, CHENG-ZHI XIE†, YAN OUYANG† and JING-YUAN XU*†

†Tianjin Key Laboratory on Technologies Enabling Development of Clinical Therapeutics and Diagnostics, School of Pharmacy, Tianjin Medical University, Tianjin, P.R. China
‡The Second Hospital of Tianjin Medical University, Tianjin, P.R. China

(*Received 28 November 2012; in final form 27 March 2013*)

Two new complexes, $[Co(L)_2]Cl\cdot(MeOH)_2$ (**1**) and $[Ni(L)_2]_4\cdot EtOH$ (**2**) (L = (*E*)-2-(amino((pyridin-2-ylmethylene)amino)methylene)maleonitrile), were synthesized and characterized by X-ray crystallography, IR, UV, and fluorescence spectroscopy. According to X-ray crystallographic studies, each metal was six-coordinate with six nitrogens from two ligands. Both complexes form two-dimensional supramolecular networks via hydrogen bonding and π–π interactions. Ultraviolet and visible spectra showed that absorptions arise from π–π^*, MLCT, and d–d electron transitions. Fluorescence spectroscopy revealed moderate intercalative binding of these two complexes with EB–DNA, with apparent binding constant (K_{app}) values of 9.14×10^5 and $3.20 \times 10^5\,M^{-1}$ for Co(III) and Ni(II) complexes, respectively. UV–visible absorption spectra showed that the absorption of DNA at 260 nm was quenched for **2** but quenched then improved for **1** with addition of complexes, tentatively attributed to the effect of the combined intercalative binding and electrostatic interaction for **1**.

Keywords: (*E*)-2-(Amino((pyridin-2-ylmethylene)amino)methylene)maleonitrile; Crystal structure; Ni(II) complex; Co(III) complex; DNA interaction

1. Introduction

Interaction of metal complexes with DNA is important in biotechnology and medicine [1–10]. Metal complexes are widely used in gene regulation, probing of DNA specific structures, mapping of protein and DNA interaction, DNA foot-printing and cancer therapy [11–24]. Schiff bases are an important class of compounds in medicinal chemistry with potential for anti-inflammatory, antibacterial, and chemotherapeutic applications [25, 26]. Schiff bases have rich coordination donors and potential to form extensive hydrogen bonding in the crystal packing lattice [27]. Metal complexes containing Schiff bases could show increased antibacterial and antiproliferative activities compared to the properties of the

*Corresponding author. Email: xujingyuan@tmu.edu.cn
[1]These authors contributed equally to this work.

metal center or coordinating ligands alone [28–30]. In an attempt to further exploit metal complexes with potential biological function in life science, our study has focused on diverse Schiff base ligands and their corresponding complexes, examining their binding mode with DNA and protein, thus disclosing possible structure–biological relevance. Herein, we report two new complexes, $[Co(L)_2]Cl\cdot(MeOH)_2$ (**1**) and $[Ni(L)_2]_4\cdot EtOH$ (**2**) (L = (*E*)-2-(amino((pyridin-2-ylmethylene)amino)methylene)maleonitrile), and competitive binding experiments to investigate the interactions of these two complexes with calf thymus DNA (CT-DNA). The results showed that both complexes replaced Ethidium bromide (EB) to bind to DNA. Red shift (or blue shift) phenomenon or hyperchromic (or subtractive) effect would be caused in the absorption of DNA when it binds with metal complexes. So, UV–visible absorption spectra were used to examine the interaction of complexes with DNA.

2. Experimental

2.1. *Materials and measurements*

Reagents were purchased commercially and used without purification. EB and CT-DNA were purchased from Sigma. IR spectra were recorded as KBr disks on a Shimadzu IR-408 infrared spectrophotometer from 4000–600 cm^{-1}, and electronic spectra were measured on a Shimadzu UV-2101PC UV–visible scanning spectrophotometer in acetonitrile. Fluorescence spectral data were obtained on a MPF-4 fluorescence spectrophotometer at room temperature.

All experiments between the complexes and CT-DNA were carried out in Tris-HCl/NaCl buffer solution (pH 7.2). CT-DNA was sufficiently free of protein, with ratio of its UV absorbance at 260 and 280 nm of 1.8–1.9. The concentration of CT-DNA was determined by employing an extinction coefficient of 6600 $M^{-1}cm^{-1}$ at 260 nm.

2.2. *Preparation of 2-amino-3-((E)-(pyridine-2-ylmethylene)amino) maleonitrile (L)*

A mixture of diaminomaleonitrile (2.16 g, 0.02 mM) and pyridine-2-carbaldehyde (1.9 mL, 0.02 mM) was dissolved in DMF (10 mL) and stirred for 0.5 h until complete dissolution occurred. Then, $K_2S_2O_8$ (3.26 g, 0.012 mM) and $KHSO_4$ (4.92 g, 0.036 mM) were added and mixed with H_2O (0.5 mL). Abruptly, the orange clear liquid turned to a yellow suspension with heat released. The solution was stirred for 4 h at room temperature. The yellow suspension was poured into water (300 mL) and slowly treated with saturated K_2CO_3 to pH 7. The yellow solid was collected by filtration and washed several times by water. The crude product was recrystallized from EtOH to give deep yellow needle crystals. Yield: 64% (2.538 g). Main IR bands (KBr, cm^{-1}): 3369 s(sh), 2928 w, 2234 m, 2195 s(sh), 1633 s(sh), 1604 m, 1587 m, 1561 m, 1463 m, 1432 m, 1369 m(br), 1232 w, 1043 w, 941 m, 780 s.

2.3. *Preparation of $[Co(L)_2]Cl\cdot(MeOH)_2$ (1)*

L (0.0788 g, 0.4 mM) was dissolved in MeOH (15 mL) and dropped into MeOH solution of $CoCl_2\cdot 6H_2O$ (0.0476 g, 0.2 mM) under stirring, to give a red-brown solution. The solution was stirred at room temperature for 4 h, then the mixture was filtered and left to

Table 1. Crystal data and structure refinement for **1** and **2**.

Complex	**1**	**2**
Empirical formula	$C_{22}H_{20}ClCoN_{10}O_2$	$C_{82}H_{54}N_{40}Ni_4O$
Formula weight	550.86	1850.49
Temperature (K)	293(2)	293(2)
Wavelength (Å)	0.71073	0.71073
Crystal system	Monoclinic	Triclinic
Space group	$P2_1/c$	*P-1*
a (Å)	8.5570(17)	13.209(2)
b (Å)	19.288(4)	17.478(3)
c (Å)	15.595(3)	19.172(3)
α (°)	90	91.1600(10)
β (°)	92.61(3)	104.035(3)
γ (°)	90	101.909(3)
V (Å^3)	2571.2(9)	4190.1(12)
Z	4	2
D_{calc} (g/cm^3)	1.423	1.467
Absorption coefficient (mm^{-1})	0.811	0.958
F(0 0 0)	1128	1892
Crystal size (mm)	0.18 × 0.15 × 0.12	0.18 × 0.16 × 0.12
Theta range for data collection	2.48–25.04	1.19–27.88
Limiting indices	$-10 \leqslant h \leqslant 10$, $-22 \leqslant k \leqslant 21$, $-18 \leqslant l \leqslant 18$	$-16 \leqslant h \leqslant 17$, $-22 \leqslant k \leqslant 22$, $-25 \leqslant l \leqslant 25$
Reflections collected/unique	21,241/4551 [R_{int} = 0.0646]	43,199/19,679 [R_{int} = 0.0417]
Completeness to θ = 25.04	99.9%	98.4%
Max. and min. transmission	0.9089 and 0.8677	0.8937 and 0.8464
Data/restraints/parameters	4551/0/330	19,679/0/1148
Goodness of fit on F^2	1.035	1.000
Final R indices [$I > 2\sigma(I)$]	R_1 = 0.0543, wR_1 = 0.1338	R_1 = 0.0398, wR_1 = 0.0736
R indices (all data)	R_1 = 0.0701, wR_2 = 0.1434	R_1 = 0.0543, wR_1 = 0.0788
Largest diff. peak (e Å^{-3})	0.527 and −0.567	0.384 and −0.530

Table 2. Selected bond lengths (Å) and angles (°) for **1**.

Bond lengths			
Co1–N1	1.953(3)	Co1–N4	1.887(3)
Co1–N5	1.891(3)	Co1–N6	1.896(3)
Co1–N7	1.887(3)	Co1–N10	1.954(3)
Bond angles			
N4–Co1–N7	176.87(12)	N4–Co1–N5	84.17(12)
N7–Co1–N5	93.70(12)	N4–Co1–N6	93.28(12)
N7–Co1–N6	84.45(12)	N5–Co1–N6	91.06(12)
N4–Co1–N1	82.65(11)	N7–Co1–N1	99.51(11)
N5–Co1–N1	166.77(11)	N6–Co1–N1	90.94(12)
N4–Co1–N10	99.66(11)	N7–Co1–N10	82.58(11)
N5–Co1–N10	89.25(12)	N6–Co1–N10	167.02(11)
N1–Co1–N10	91.72(11)		

stand at room temperature for slow evaporation, and dark-red crystals of complex suitable for X-ray analysis were collected after several days. Yield: 39% (0.0429 g). IR (KBr, cm^{-1}): 3411 m(br), 2956 m(br), 2358 w, 2193 s(sh), 1600 m, 1572 m, 1542 s, 1510 s(sh), 1464 m, 1250 s, 1154 m, 787 m, 441 m.

Table 3. Selected bond lengths (Å) and angles (°) for **2**.

Bond lengths			
Ni1–N16	2.0332(16)	Ni1–N13	2.0354(16)
Ni1–N17	2.0767(16)	Ni1–N12	2.0925(17)
Ni1–N15	2.1223(16)	Ni1–N14	2.1344(15)
Ni2–N4	2.0276(17)	Ni2–N9	2.0292(16)
Ni2–N3	2.0705(16)	Ni2–N8	2.0715(16)
Ni2–N30	2.1213(16)	Ni2–N5	2.1297(16)
Ni3–N33	2.0291(16)	Ni3–N37	2.0311(16)
Ni3–N38	2.0814(16)	Ni3–N34	2.0885(16)
Ni3–N36	2.1297(15)	Ni3–N35	2.1302(16)
Ni4–N22	2.0362(16)	Ni4–N26	2.0385(16)
Ni4–N25	2.0631(16)	Ni4–N23	2.0722(17)
Ni4–N24	2.1103(16)	Ni4–N29	2.1397(16)
Bond angles			
N16–Ni1–N13	175.39(6)	N16–Ni1–N17	79.12(6)
N13–Ni1–N17	102.02(6)	N16–Ni1–N12	105.29(6)
N13–Ni1–N12	79.19(6)	N17–Ni1–N12	91.34(6)
N16–Ni1–N15	77.91(6)	N13–Ni1–N15	100.95(6)
N17–Ni1–N15	157.02(6)	N12–Ni1–N15	93.76(6)
N16–Ni1–N14	97.66(6)	N13–Ni1–N14	77.83(6)
N17–Ni1–N14	94.19(6)	N12–Ni1–N14	157.01(6)
N15–Ni1–N14	89.80(6)	N4–Ni2–N9	175.05(6)
N4–Ni2–N3	79.91(6)	N9–Ni2–N3	100.98(6)
N4–Ni2–N8	104.84(6)	N9–Ni2–N8	80.05(7)
N3–Ni2–N8	90.80(6)	N4–Ni2–N30	97.05(6)
N9–Ni2–N30	78.07(6)	N3–Ni2–N30	92.48(6)
N8–Ni2–N30	158.10(7)	N4–Ni2–N5	77.94(6)
N9–Ni2–N5	101.25(6)	N3–Ni2–N5	157.77(7)
N8–Ni2–N5	93.02(6)	N30–Ni2–N5	92.09(6)
N33–Ni3–N37	176.21(6)	N33–Ni3–N38	101.67(6)
N37–Ni3–N38	79.97(6)	N33–Ni3–N34	79.48(6)
N37–Ni3–N34	103.85(6)	N38–Ni3–N34	95.09(6)
N33–Ni3–N36	100.42(6)	N37–Ni3–N36	77.88(6)
N38–Ni3–N36	157.86(6)	N34–Ni3–N36	90.38(6)
N33–Ni3–N35	77.92(6)	N37–Ni3–N35	98.62(6)
N38–Ni3–N35	93.03(6)	N34–Ni3–N35	157.11(6)
N36–Ni3–N35	90.10(6)	N22–Ni4–N26	171.93(6)
N22–Ni4–N25	97.13(6)	N26–Ni4–N25	79.84(6)
N22–Ni4–N23	79.49(7)	N26–Ni4–N23	107.98(7)
N25–Ni4–N23	92.01(6)	N22–Ni4–N24	78.00(7)
N26–Ni4–N24	94.53(6)	N25–Ni4–N24	91.42(6)
N23–Ni4–N24	157.48(7)	N22–Ni4–N29	105.56(6)
N26–Ni4–N29	77.39(6)	N25–Ni4–N29	157.21(7)
N23–Ni4–N29	94.15(6)	N24–Ni4–N29	91.22(6)

2.4. *Preparation of $[Ni(L)_2]_4$·EtOH (2)*

A solution of L (0.0788 g, 0.4 mM) in EtOH (15 mL) was added to a solution of $Ni(OAc)_2·4H_2O$ (0.0498 g, 0.2 mM) in EtOH (15 mL) and the mixture was continuously stirred for 4 h. The red-brown reaction mixture was filtered, left to stand at room temperature for slow evaporation, and deep black-red crystals of complex suitable for X-ray analysis were collected after several days. Yield: 43% (0.0398 g). IR (KBr, cm^{-1}): 3370 m, 3344 m, 2364 w, 2173 s(sh), 1598 m, 1546 s, 1509 s(sh), 1461 s(sh), 1410 s(sh), 1244 m, 1152 m, 771 m, 437 w.

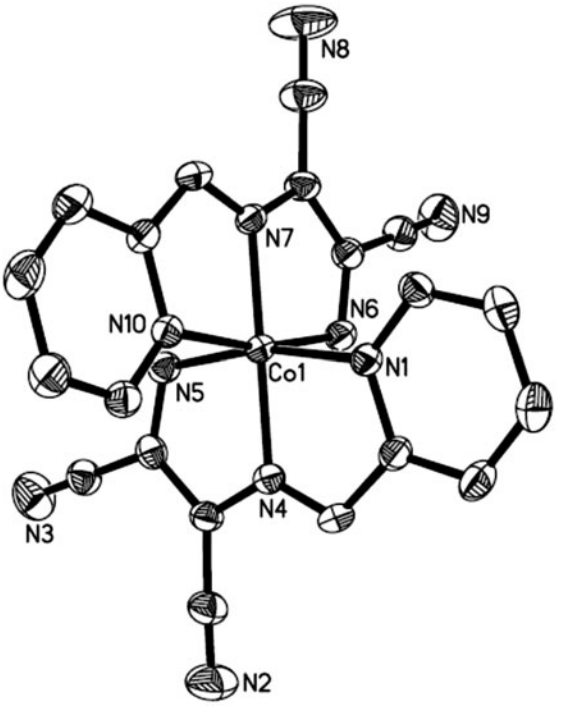

Figure 1. An ORTEP view of **1**. The non-coordinated chlorides, solvent and hydrogens are omitted for clarity.

2.5. *Structure determination*

The diffraction data of the complexes were determined on a Rigaku Saturn CCD diffractometer using graphite-monochromated MoKα radiation ($\lambda = 0.71073$ Å) with the ω–2θ scan technique. An empirical absorption correction was applied to the raw intensities. The structures were solved by direct methods (SHELXS-97) and refined with full matrix least-squares on F^2 using SHELXL-97. Experimental conditions for diffraction analysis, structural analysis, correction method, and crystal data are listed in table 1. Selected bond lengths and angles are provided in tables 2 and 3. Crystallographic data for the structures reported in this article have been deposited at the Cambridge Crystallographic Data Center, CCDC No. 906,671 and 906,672. Copies of the data can be obtained free of charge on application to CCDC, 12 Union Road, Cambridge CB2 1EZ, UK [Fax: +44 1223 336–033; E-mail: deposit@ccdc.cam.ac.uk].

3. Results and discussion

3.1. *Crystal study*

Complex **1** crystallizes in the monoclinic system with space group $P2_1/c$, $Z = 4$. The structure of **1** consists of one $[CoL_2]^+$ (see figure 1), one uncoordinated Cl^-, and two methanols. Each Co(III) is coordinated by six nitrogens from two ligands, forming a slightly distorted octahedral geometry. The two L coordinate tridentate exhibiting two

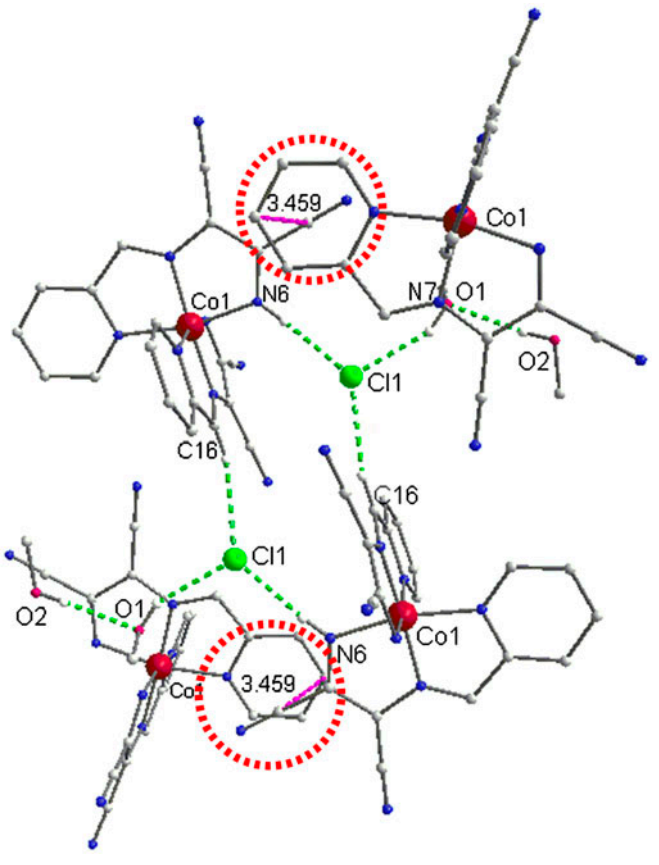

Figure 2. Hydrogen bonds (dotted lines) and $\pi\cdots\pi$ stacking (dotted circles) viewed down the *a*-axis resulting in a 2-D structure for **1**.

slightly distorted planes with dihedral angles of 88.8°. Each plane is constructed by all 10 carbons and five nitrogens of L as well as one Co, in which the basal atoms deviate from their mean plane by *ca.* ±0.0236 and ±0.0310 Å, respectively, and the metal is displaced out of the plane by 0.0360 and 0.0818 Å, respectively. The uncoordinated Cl^- connects with one nitrogen (N6) of a terminal amino group of L from one $[CoL_2]^+$ at 3.1098(30) Å, one carbon (C16) from another $[CoL_2]^+$ unit at 3.5052(39) Å, and one oxygen (O1) from one methanol at 3.0399(36) Å through hydrogen bonds. The angles of these hydrogen bonds are 169.774(165)°, 152.537(231)°, and 152.865(242)°, respectively. Additional hydrogen bonds O–H···O with bond length 2.8374(58) Å and angle 165.371(339)° exist between two methanols; thus, all hydrogen bonds make $[Co(L)_2]Cl\cdot(MeOH)_2$ appear in pairs. One of two conjugated linear maleonitrile groups of ligand faces the pyridine ring of the neighbor $[CoL_2]^+$ with line-to-plane distance of *ca.* 3.458 Å, showing distinct $\pi\cdots\pi$ interactions. Thus, hydrogen bonds and $\pi\cdots\pi$ stacking together result in the 2-D structure in crystals of **1** as depicted in figure 2.

Complex **2** was triclinic with space group *P-1*, $Z=2$. The unit cell of the complex contains four $[NiL_2]$ neutral molecules, whose coordination geometries are similar but with slightly different bond lengths and angles, and one solvent ethanol. An ORTEP drawing of

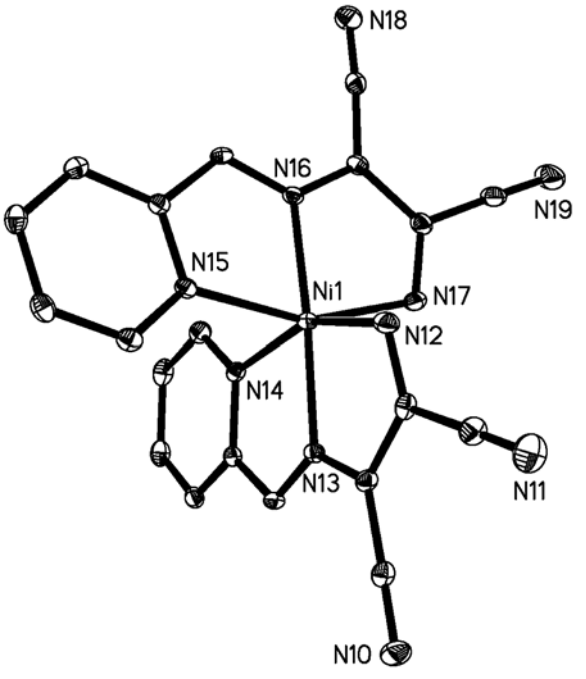

Figure 3. An ORTEP view of one $[Ni(L)_2]$ in **2**. The non-coordinated solvent and hydrogens are omitted for clarity.

one $[NiL_2]$ neutral unit of **2** is depicted in figure 3. X-ray diffraction analysis revealed that $[NiL_2]$ has similar coordination environment with six nitrogens from two ligands constituting a distorted octahedral structure. Two ligands cocoordinated to one Ni(II) forming two big planes with dihedral angles of 85.8°, and basal atoms deviating from their mean plane by *ca.* ±0.0365 and ±0.0485 Å, respectively; the metal is displaced out of the plane by 0.0049 and 0.1052 Å, respectively. The packing diagram (figure 4(a)) shows intermolecular hydrogen bonds between nitrogen of $–NH_2$ and maleonitrile group, such as $N12_{amine}$–$H12B\cdots N28_{maleonitrile}$ at 3.086 Å, $N25_{amine}$–$H25B\cdots N20_{maleonitrile}$ at 3.185 Å, and one carbon (C49) of pyridine ring and N (N1) of $–NH_2$ group, from different $[NiL_2]$ units at 3.435 Å, with corresponding hydrogen bond angles 164.3°, 163.5°, and 158.2°, respectively. Two pyridine rings of two ligands face the pyridine ring of their contiguous $[NiL_2]$ pair with plane-to-plane distance of *ca.* 3.815(36) and 3.659(31) Å, respectively, showing distinct $\pi\cdots\pi$ interactions (figure 4(b)).

3.2. *Spectroscopic properties*

IR spectra of the complexes display absorptions at 1600–1400 and $900-700\,cm^{-1}$, consistent with pyridine. The band at $3400\,cm^{-1}$ can be assigned to ν(NH). Two sharp bands in the $2100–2300\,cm^{-1}$ region suggest the presence of ν(CN). The band at about $440\,cm^{-1}$ can be assigned to ν(M–N) [31].

The ultraviolet and visible spectra (200–900 nm, acetonitrile solution) showed two very strong absorption bonds at $46{,}296\,cm^{-1}$ (216 nm, $\varepsilon = 3.08 \times 10^4\,L\,mol^{-1}\,cm^{-1}$),

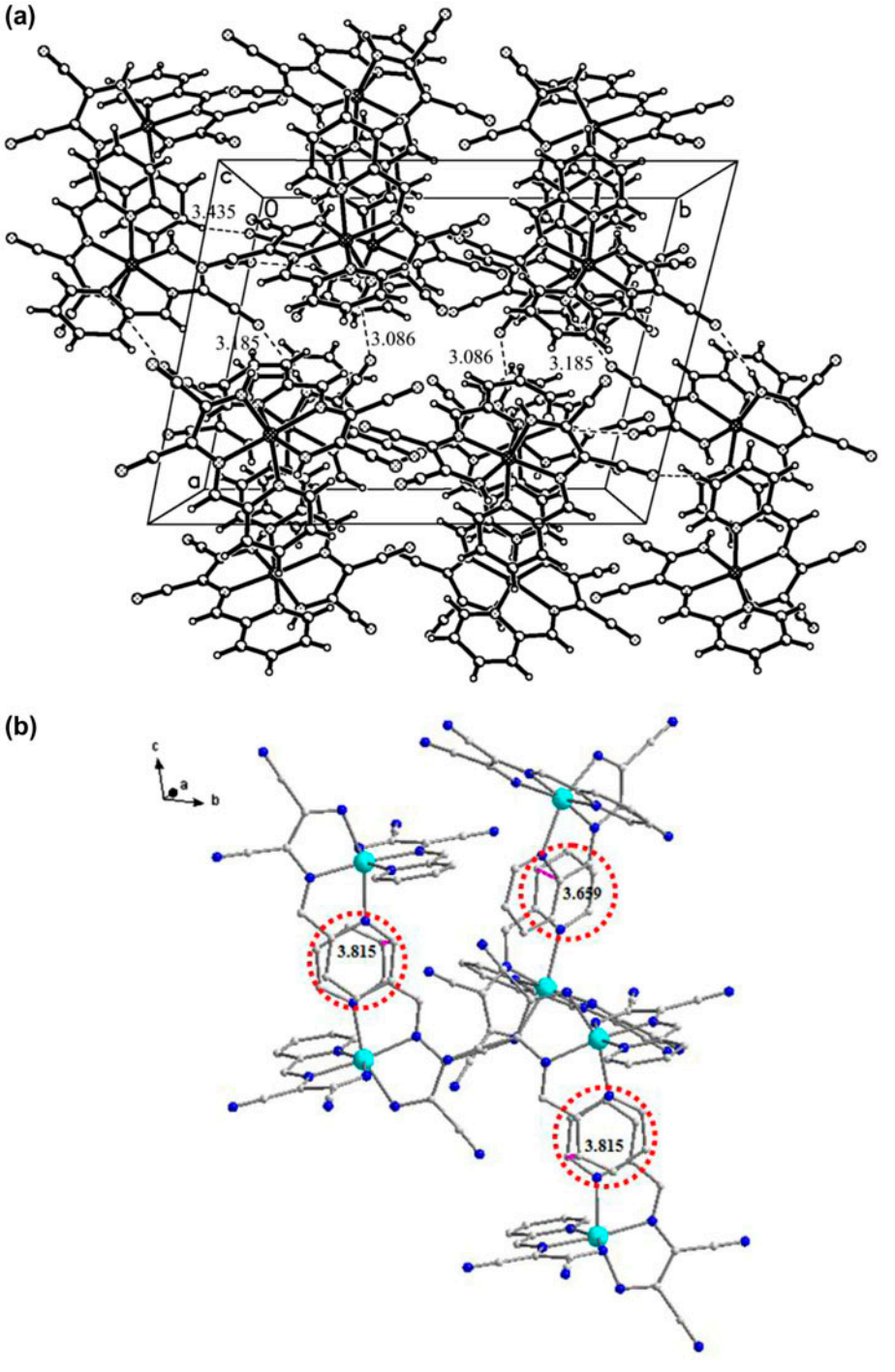

Figure 4. Packing diagram of **2** viewed along the *a*-axis (a) and *b*-axis (b) showing hydrogen bonds and $\pi\cdots\pi$ interactions, respectively.

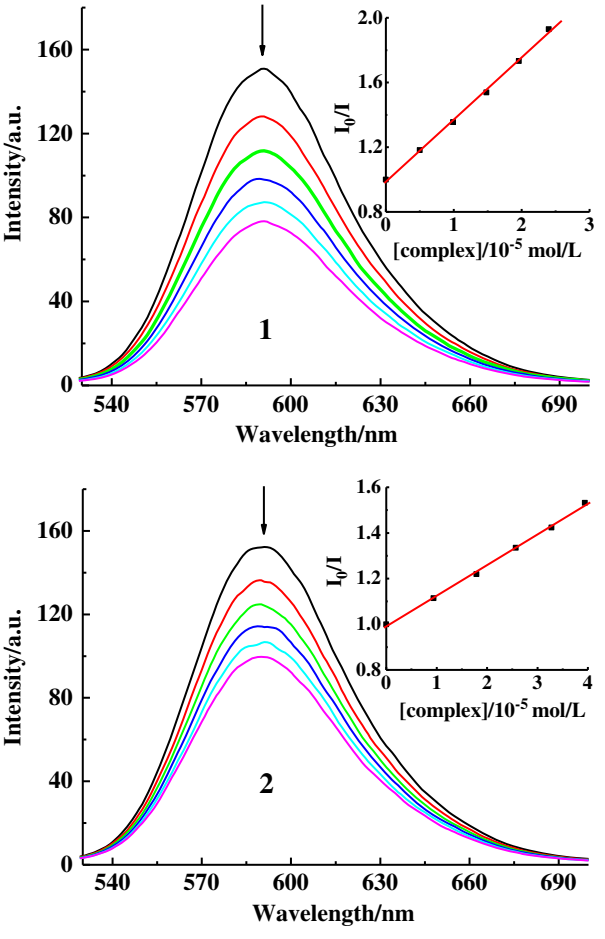

Figure 5. Fluorescence quenching curves of EB bound to DNA by **1** ([complex] = 0–2.4 × 10^{-5} M, upper) and **2** ([complex] = 0–3.94 × 10^{-5} M, lower). The arrow shows the intensity changes on increasing complex concentration. Inset: Plot of I_0/I *vs.* [complex], λ_{ex} = 510 nm.

37,037 cm^{-1} (270 nm, $\varepsilon = 1.74 \times 10^4$ L mol^{-1} cm^{-1}) for **1** and 38,023 cm^{-1} (263 nm, $\varepsilon = 1.82 \times 10^4$ L mol^{-1} cm^{-1}) for **2**, which may be attributed to $\pi \rightarrow \pi^*$ electronic transition of the ligand. For **1**, one shoulder at 30,395 cm^{-1} (329 nm, $\varepsilon = 1.33 \times 10^4$ L mol^{-1} cm^{-1}) may be from Co(III)→L MLCT charge-transfer transition. A very strong absorption at 30,675 cm^{-1} (326 nm, $\varepsilon = 1.42 \times 10^4$ L mol^{-1} cm^{-1}) for **2** may be ascribed to Ni(II)→L MLCT charge-transfer transition. Complex **1** showed a strong broad absorption at 19,960 cm^{-1} (501 nm, $\varepsilon = 1.22 \times 10^4$ L mol^{-1} cm^{-1}), attributable to the symmetry forbidden d–d transition of Co(III) ($^1A_{1g} \rightarrow {}^1T_{1g}$, $^1A_{1g} \rightarrow {}^1T_{2g}$) and 20,747 cm^{-1} (482 nm, $\varepsilon = 3.01 \times 10^4$ L mol^{-1} cm^{-1}) for **2** is the d–d transition of the Ni(II) ($^3A_{2g} \rightarrow {}^3T_{1g}$, $^3A_{2g} \rightarrow {}^1A_{1g}$, $^1T_{2g}$).

To further clarify the binding of complexes with DNA, the EB–DNA fluorescence quenching spectral experiment was carried out by adding solution of **1** and **2** at different concentrations to the samples, containing 2.4 μM EB and 47.6 μM CT-DNA. As shown in figure 5, the complexes were excited at 510 nm, and emission was recorded at 520–700 nm. The fluorescence of EB–DNA solution was quenched by addition of **1** and **2**, demonstrating

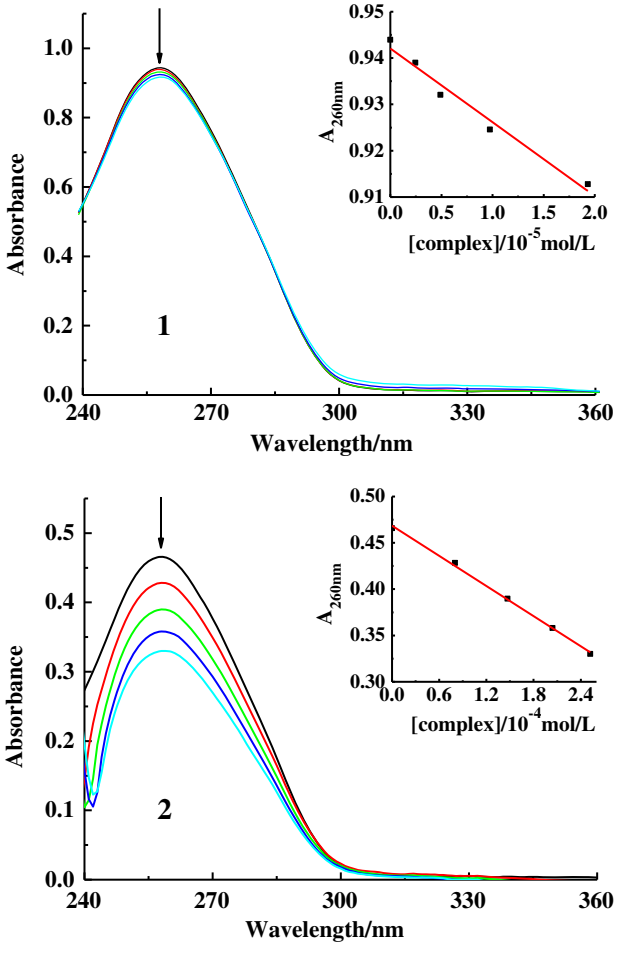

Figure 6. The effect of the addition of **1** ([complex] = 0–1.93×10^{-5} M) and **2** ([complex] = 0–2.52×10^{-4} M) on UV–visible spectra of the DNA solution. Inset plot shows the DNA absorbance at around 260 nm changes with increasing complex concentration.

that both complexes could competitively bind to DNA with EB. Reduction in the emission intensity offered a measure of the interactions of the two complexes with DNA. According to the classical Stern–Volmer equation [32] $I_0/I = 1 + K\,[Q]$, the binding capacity of the complexes with DNA was surveyed from the slope of straight line acquired for the fluorescence intensity *versus* the complex concentration. According to the equation $K_{EB}[EB] = K_{app}[complex]$, $K_{EB} = 1.0 \times 10^7\,M^{-1}$ ([EB] = 2.4 μM), the apparent binding constants (K_{app}) were counted to be 9.14×10^5 for **1** and 3.20×10^5 for **2**, which were less than the classical binding constant ($K_{EB} = 10^7\,M^{-1}$).

3.3. *Effect of Co(III) and Ni(II) complexes on UV absorption of DNA*

DNA has a maximum absorption normally at 260 nm in UV–visible absorption spectra. Conformational changes of DNA give red shift and the hypochromic effect of the

absorption; however, hyperchromic effect would occur when the double helix of DNA is destroyed [33, 34]. Absorption titration experiments were executed at fixed concentration of CT-DNA. The absorption band of the DNA at 260 nm was red-shifted by 2 nm (figure 6) and quenched by 29% with the increasing amount of **2**; the absorption was only quenched by 3% when **1** (10^{-3} ML^{-1}) was added to 40 μL, and if farther **1** was kept added, the absorption band of DNA increased instead, suggesting that **1** might take different DNA interaction mechanism from **2**, owing to the existence of cationic in **1** but neutral in **2**. So, the phenomenon generated by **1** might arise from electrostatic interaction between DNA and Co(III) unit in addition to intercalation to binding discussed above.

4. Conclusions

Two mononuclear metal complexes were synthesized and characterized by single-crystal X-ray diffraction, IR, UV, and fluorescence spectroscopy. Each metal of both complexes was six-coordinate with six nitrogens from two ligands. Ultraviolet and visible spectra showed absorptions from π–π^*, MLCT, and d–d electron transitions. DNA binding of the complexes was investigated by fluorescence spectroscopy with apparent binding constant (K_{app}) values of 9.14×10^5 and 3.20×10^5 M^{-1} for Co(III) and Ni(II) complexes, respectively, comparable to those reported for cobalt and nickel complexes with a tetradentate Schiff base [35–37]. The UV absorption band of DNA at 260 nm was quenched for **2** but quenched and then improved for **1** with the addition of complexes, suggesting different DNA mechanism between **1** and **2**. The exact mechanism is not well understood and warrants further research.

Acknowledgement

This work was supported by National Natural Science Foundation of China (No. 20971099).

References

[1] E.L. Hegg, J.N. Burstyn. *Coord. Chem. Rev.*, **173**, 133 (1998).
[2] S. Aoki, E. Kimura. *Chem. Rev.*, **104**, 769 (2004).
[3] L.F. Tan, X.L. Liang, X.H. Liu. *J. Inorg. Biochem.*, **103**, 441 (2009).
[4] Y.J. Liu, C.H. Zeng, H.L. Huang, L.X. He, F.H. Wu. *Eur. J. Med. Chem.*, **45**, 564 (2010).
[5] Y.J. Liu, C.H. Zeng, Z.H. Liang, J.H. Yao, H.L. Huang, Z.Z. Li, F.H. Wu. *Eur. J. Med. Chem.*, **45**, 3087 (2010).
[6] X.H. Zou, B.H. Ye, H. Li, Q.L. Zhang, H. Chao, J.G. Liu, L.N. Ji, X.Y. Li. *J. Biol. Inorg. Chem.*, **6**, 143 (2001).
[7] C.F. Zhou, X.S. Du, H. Li. *Bioelectrochemistry*, **70**, 446 (2007).
[8] B. Peng, H. Chao, B. Sun, H. Li, F. Gao, L.N. Ji. *J. Inorg. Biochem.*, **101**, 404 (2007).
[9] X.W. Liu, J.L. Lu, Y.D. Chen, L. Li, D.S. Zhang. *Inorg. Chem. Commun.*, **13**, 449 (2010).
[10] H.P. Aishakhanam, P.B. Raghavendra, N.N. Ganesh, S.F. Christopher, B.G. Kalagouda. *Polyhedron*, **34**, 149 (2012).
[11] D.S. Sigman, T.W. Bruice, A. Mazumder, C.L. Sutton. *Acc. Chem. Res.*, **26**, 98 (1993).
[12] D.S. Sigman, A. Mazumder, D.M. Perrin. *Chem. Rev.*, **93**, 2295 (1993).
[13] B. Meunier. *Chem. Rev.*, **92**, 1411 (1992).
[14] C. Metcalfe, J.A. Thomas. *Chem. Soc. Rev.*, **32**, 215 (2003).
[15] K.E. Erkkila, D.T. Odom, J.K. Barton. *Chem. Rev.*, **99**, 2777 (1999).

[16] B. Armitage. *Chem. Rev.*, **98**, 1171 (1998).
[17] D.R. McMillin, K.M. McNett. *Chem. Rev.*, **98**, 1201 (1998).
[18] H.T. Chifotides, K.R. Dunbar. *Acc. Chem. Res.*, **38**, 146 (2005).
[19] E.R. Jamieson, S.J. Lippard. *Chem. Rev.*, **99**, 2467 (1999).
[20] F. Gao, H. Chao, F. Zhou, Y.X. Yuan, B. Peng, L.N. Ji. *J. Inorg. Biochem.*, **100**, 1487 (2006).
[21] A. Jain, C. Slebodnick, B.S.J. Winkel, K.J. Brewer. *J. Inorg. Biochem.*, **102**, 1854 (2008).
[22] A.G. Zhang, Y.Z. Zhang, Z.M. Duan, K.Z. Wang. *Inorg. Chem.*, **50**, 6425 (2011).
[23] Y.M. Chen, Y.J. Liu, Q. Li, K.Z. Wang. *J. Inorg. Biochem.*, **103**, 1395 (2009).
[24] C.C. Ju, A.G. Zhang, C.L. Yuan, X.L. Zhao, K.Z. Wang. *J. Inorg. Biochem.*, **105**, 435 (2011).
[25] A.W. Tai, E.J. Lien, M.M.C. Lai, T.A. Khwaja. *J. Med. Chem.*, **27**, 236 (1984).
[26] P.H. Wang, J.G. Keck, E.J. Lien, M.M.C. Lai. *J. Med. Chem.*, **33**, 608 (1990).
[27] P.A. Vigato, S. Tamburini. *Coord. Chem. Rev.*, **248**, 1717 (2004).
[28] C.A. Bolos, G.S. Nikolov, L. Ekateriniadou, A. Kortsaris, D.A. Kyriakidis. *Met.-Based Drugs*, **5**, 323 (1998).
[29] A.T. Chaviara, P.J. Cox, K.H. Repana, R.M. Papi, K.T. Papazisis, D. Zambouli, A.H. Kortsaris, D.A. Kyriakidis, C.A. Bolos. *J. Inorg. Biochem.*, **98**, 1271 (2004).
[30] A.T. Chaviara, P.J. Cox, K.H. Repana, A.A. Pantazaki, K.T. Papazisis, A.H. Kortsaris, D.A. Kyriakidis, G.S. Nikolov, C.A. Bolos. *J. Inorg. Biochem.*, **99**, 467 (2005).
[31] L. Gupta, S. Chandra. *Spectrochim. Acta, Part A*, **71**, 496 (2008).
[32] J.R. Lakowicz, G. Webber. *Biochemistry*, **12**, 4161 (1973).
[33] A. Manna, S. Chakravorti. *J. Phys. Chem. B*, **116**, 5226 (2012).
[34] H.H. Li, X.Y. Bu, J. Lu, C.Z. Xu, X.L. Wang, X.D. Yang. *Spectrochim. Acta, Part A*, **107**, 227 (2013).
[35] A. Patra, S. Sen, S. Sarkar, E. Zangrando, P. Chattopadhyay. *J. Coord. Chem.*, **65**, 4096 (2012).
[36] N. Raman, K. Pothiraj, T. Baskaran. *J. Coord. Chem.*, **64**, 4286 (2011).
[37] N. Raman, K. Pothiraj, T. Baskaran. *J. Coord. Chem.*, **64**, 3900 (2011).